Nonrigid Versus Rigid Registration of Thoracic ^{18}F-FDG PET and CT in Patients with Lung Cancer: An Intraindividual Comparison of Different Breathing Maneuvers

Aleksandar Grgic[1], Ursula Nestle[1,2], Andrea Schaefer-Schuler[1], Stephanie Kremp[3], Elena Ballek[1], Jochen Fleckenstein[3], Christian Rübe[3], Carl-Martin Kirsch[1], and Dirk Hellwig[1]

[1]Department of Nuclear Medicine, Saarland University Medical Center, Homburg/Saar, Germany; [2]Department of Radio-Oncology, University Hospital Freiburg, Freiburg, Germany; and [3]Department of Radio-Oncology, Saarland University Medical Center, Homburg/Saar, Germany

In lung cancer, ^{18}F-FDG PET, CT, and ^{18}F-FDG PET/CT are used for noninvasive staging and therapy planning. Even with improved image registration techniques—especially in the modern hybrid PET/CT scanners—inaccuracies in the fusion process may occur, leading to errors in image interpretation. The aim of this study was to investigate by an intraindividual analysis whether, in comparison with a rigid algorithm, a nonrigid registration algorithm improves the quality of fusion between ^{18}F-FDG PET and CT. **Methods:** Sixteen patients with histologically proven non–small cell lung cancer underwent a thoracic ^{18}F-FDG PET acquisition in radiotherapy treatment position and 3 CT acquisitions (expiration, inspiration, and mid breath-hold) on the same day. All scans were registered with rigid and nonrigid procedures, resulting in 6 fused datasets: rigid inspiration, rigid expiration, rigid mid breath-hold, nonrigid inspiration, nonrigid expiration, and nonrigid mid breath-hold. The quality of alignment was assessed by 3 experienced readers at 8 anatomic landmarks: lung apices, aortic arch, heart, spine, sternum, carina, diaphragm, and tumor using an alignment score ranging from 1 (no alignment) to 5 (exact alignment). **Results:** Nonrigid PET/CT showed better alignment than rigid PET/CT (3.5 ± 0.7 vs. 3.3 ± 0.7, $P < 0.001$). Regarding the breathing maneuver, no difference between nonrigid mid breath-hold and rigid mid breath-hold was observed. In contrast, the alignment quality significantly improved from rigid expiration to nonrigid expiration (3.4 ± 0.7 vs. 3.6 ± 0.7, $P < 0.001$) and from rigid inspiration to nonrigid inspiration (3.1 ± 0.7 vs. 3.3 ± 0.7, $P < 0.001$). With regard to individual landmarks, an improvement in fusion quality through the use of nonrigid registration was obvious at the lung apices, carina, and aortic arch. **Conclusion:** The alignment quality of thoracic ^{18}F-FDG PET/CT exhibits a marked dependence on the breathing maneuver performed during the CT acquisition, as demonstrated in an intraindividual comparison. Nonrigid registration is a significant improvement over rigid registration if the CT is performed during full inspiration or full expiration. The best fusion results are obtained with the CT performed at mid breath-hold using rigid registration, without an improvement using nonrigid algorithms.

Key Words: non–small cell lung carcinoma (NSCLC); spiral computed tomography; positron emission tomography; image registration; computer-assisted image analysis

Lung cancer is responsible for 15% of all newly occurring cases of cancer and is the most common cause of cancer death in the United States (*1*). As the prognosis is strongly influenced by the stage of the disease, accurate staging is of the utmost importance and determines the best treatment approach (*2*). PET using ^{18}F-FDG is currently the most accurate imaging modality in the evaluation of non–small cell lung cancer (*3,4*). However, spatial resolution is lower for PET images than for anatomic images. This problem has been overcome by the combination of the functional PET image and the anatomic CT image, using both integrated PET/CT scanners and software-based image fusion (*5–7*). Furthermore, fused CT data are of use for attenuation correction of PET image data, especially in the context of PET/CT (*7*). Even in modern hybrid PET/CT systems, misregistration of PET and CT volumes may occur, especially in the lower part of the thorax, with impact on thoracic and cardiac PET (*8,9*).

Accurate image fusion is necessary not only in correctly establishing the diagnosis and following up patients but also in determining standardized uptake values and plan-

ning radiotherapy (*10,11*). Previous studies have reported various techniques to minimize misalignment of coregistration (*12–14*). Under the conditions of clinical routine, the best matching between PET and CT is achieved through performing breath-hold CT during normal expiration (*12,13*) or at mid breath-hold (*14*).

Besides different respiratory techniques, additional registration algorithms may be applied to the image data to further improve the fusion quality (*15*). In general, software-based image registration may be either linear (rigid) or nonlinear (elastic or nonrigid), depending on whether the algorithm elastically transforms data (*16*). Prior studies used registration methods based on a rigid-body assumption (*13,14,17*). Although in the case of cranial imaging this assumption can be applied, the situation for extracranial imaging is more challenging because of respiratory and cardiac movement (*16*). Nonrigid algorithms were introduced to solve at least some of the problems caused by intended and unintended patient motion (*18–20*). However, the limited clinical validation of these methods restricts their clinical use (*21*).

To the best of our knowledge, there are only few data assessing the performance of image fusion by comparison of both rigid and nonrigid algorithms for PET and CT datasets acquired in the same patients (*19,20*). The purpose of this study was therefore to analyze intraindividually whether, in comparison to a rigid algorithm, a nonrigid algorithm can improve the quality of image fusion in patients with non–small cell lung cancer.

MATERIALS AND METHODS

Patients

This retrospective study included 16 consecutive radiotherapy candidates with non–small cell lung cancer (12 men, 4 women; mean age, 65 ± 8 y; range, 45–75 y). For the PET and CT examinations, all patients gave informed consent as obliged by national law.

PET Acquisition

All patients underwent thoracic ^{18}F-FDG PET in the radiotherapy position with arms elevated above the head, as described previously (*14*). All scans were started 160 min after injection of 250 MBq of ^{18}F-FDG. The patients were advised to fast at least 6 h before examination, and their blood glucose level was less than 150 mg/dL. For all examinations, an ECAT-ART PET scanner (CTI/Siemens) was used. The total field of view of 28.2 cm comprised 2 overlapping bed positions, each having a 16.4-cm field of view (emission scan time, 10 min/bed position). After the emission scan, attenuation correction was applied using a postinjection transmission scan (using two ^{137}Cs point sources) acquired in the identical position (hot transmission live time, 192 s/bed position). Attenuation-corrected image reconstruction was performed using an iterative reconstruction method (ordered-subsets expectation maximization with 2 iterations, 4 subsets, and 128×128 pixels of 5.1 mm).

CT Acquisition

Spiral CT of the chest (Elscint TWIN FLASH CT, 5-mm slice thickness, pitch of 1.2, 512×512 matrix, craniocaudal scanning direction, and standard reconstruction algorithm) was performed with patient positioning identical to that during the PET scan. To verify that the patient was positioned identically for the 2 scans, we used a laser localizer, skin markings, and photo-documentation of the position during the PET scan, and both the PET and the CT scans were obtained on a flat table with a positioning system identical to that used in the radiotherapy department. All PET and CT scans were performed on a same day; the time difference between the acquisitions varied between 4 and 6 h depending on the availability of the scanners. The CT acquisitions were of the whole lung from the apex to the bases and used 3 breathing maneuvers: full inspiration, full expiration, and mid breath-hold as described in the prior report (*14*). The correct performance of different breathing maneuvers was verified by measurement of the maximal distance between the apex and diaphragm on both sides of the lung and the maximal distance between the caudal margin of the tumor and the diaphragm, as well as the superior margin of the tumor and the apex, as described in the prior report (*14*). Furthermore, tumor motion was measured in the lateral direction using the middle of the spine as a point of reference, assuming that the spine position did not change during breathing maneuvers.

Image Registration

CT and PET data were transferred to a workstation (Hermes Medical Solutions) for further analysis and image registration. For the rigid registration, a rigid linear algorithm based on normalized mutual information was applied to the datasets using the following parameters: accuracy of 0.1%, a discard difference of less than 5.0%, an iteration limit of 1,000, and the original pixel size without voxel interpolation. In cases of significant misalignment, further manual improvement and fine-tuning was attempted, but only rigid translations with focus on the best compromise between landmarks were applied. This procedure has been reported to improve the anatomic fusion results over the results obtained with automatic registration only (*22*). The CT data were loaded as the primary fixed dataset, and the PET data were loaded as the secondary dataset. For further analysis, the resulting image data were simultaneously displayed as individual and fused images.

For nonrigid registration, software provided with the Hermes workstation (Multimodality Tool) was used. In this procedure, transmission and attenuation-corrected emission scans were registered first using the rigid linear algorithm based on normalized mutual information. This step compensated for possible movement of a patient between these 2 scans. Thereafter, the same algorithm was applied to register this fusion pair with the CT scan. After this initial step of rigid registration of these 3 scans, a nonlinear automated warping method using a thin-plate spline algorithm was applied to the data (*20*). The combined use of emission and transmission scans allows for a high degree of initial convergence and full automation of the algorithm (*20*).

During this process, 6 different datasets were built: 3 rigid PET/CT datasets (PET plus CT inspiration, PET plus CT expiration, and PET plus CT mid breath-hold) and 3 nonrigid PET/CT datasets (PET plus CT inspiration, PET plus CT expiration, and PET plus CT mid breath-hold). For further analysis, the resulting image datasets were renamed using pseudonyms and then simultaneously displayed as individual and fused images.

Analysis of Fusion Images

The 6 registered datasets of each patient were analyzed for quality of alignment at 8 anatomic landmarks: lung apices, aortic arch, heart, spine, carina tracheae, sternum, diaphragm/liver, and lung tumor/mass. The quality of alignment was rated on a scale of 1 (complete lack of alignment) to 5 (exact alignment), using a modification of the method of Krishnasetty et al. (Table 1) (17). Images were analyzed and scored independently by 3 experienced board-certified nuclear medicine physicians (one also being a radiologist), who have extensive experience in reading PET, CT, and PET/CT images. The reviewers were unaware of the breathing maneuver, patient identity, or registration method.

The patients were classified according to the location of the tumor within the lung parenchyma and the neighborhood affected (23). The first group included patients with tumors surrounded by lung or visceral pleura, without extension into the chest wall or mediastinum. The second group included patients with tumors invading the hilum, heart, or great vessels, with or without atelectasis (23). Further subclassification was based on anatomic allocation into the upper lobe or lower lobe.

Statistical Analysis

Alignment scores were compared between rigid and nonrigid PET/CT datasets using the Mann–Whitney U test. Differences between the mean values obtained from all 3 readers and all examinations with regard to anatomic landmarks and anatomic tumor location were evaluated with ANOVA. Multiplicity correction was performed using the Tukey method. Differences between breathing phases with regard to tumor and diaphragm motion were evaluated with the Mann–Whitney U test.

Differences between the registered nonrigid and rigid PET/CT datasets for all anatomic landmarks were rated using a Wilcoxon signed rank test.

Generalized κ-statistics were used to assess interobserver variability among the 3 readers based on analysis with respect to all anatomic landmarks and both datasets (24). In the previous work, we evaluated interobserver variability (14) among the 3 readers using weighted κ-statistics. Because we were now evaluating the same datasets again (rigid PET/CT), we evaluated intraobserver variability to test the reproducibility of the alignment score. To analyze intraobserver variability, we used the Cohen κ.

κ measures agreement beyond that expected to be chance alone. κ-Values of more than 0.75 indicate excellent agreement beyond chance; κ-values of 0.40–0.75 indicate fair to good agreement beyond chance; and κ-values of less than 0.40 indicate poor agreement. The results of the κ-analysis are summarized as the κ-value and P value, which determines whether the agreement is better than chance alone.

For the generalized κ-statistics, a Microsoft Excel spreadsheet was used. For the Wilcoxon signed rank test, Mann–Whitney U test, ANOVA with multiplicity correction (Tukey method), and Cohen κ, a statistical software package (SPSS, release 17; SPSS Inc.) was used. All values are expressed as mean ± SD unless otherwise indicated. A P value of less than 0.05 was considered statistically significant.

RESULTS

Comparison of Rigid and Nonrigid PET/CT

The fusion score averaged over all anatomic landmarks in all nonrigid PET/CT datasets (regardless of breathing protocol and observer) was better for nonrigid than rigid registration (nonrigid, 3.5 ± 0.7; rigid, 3.3 ± 0.7; $P <$ 0.001).

Effect of Breathing Maneuvers and Different Anatomic Positions

Table 2 compares fusion quality between rigid and nonrigid registration. Analyzing the fusion quality at the individual landmarks (regardless of breathing protocol), we found a highly significant improvement in fusion performance in the lung apices (rigid, 3.2 ± 0.7; nonrigid, 3.6 ± 0.7; $P <$ 0.001) and at the carina tracheae (rigid, 3.3 ± 0.6; nonrigid, 3.6 ± 0.6; $P <$ 0.001). Also, significantly better fusion was observed for the aortic arch (rigid, 3.3 ± 0.6; nonrigid, 3.5 ± 0.5; $P =$ 0.01). At the remaining landmarks, similar or slightly better fusion was observed for the nonrigid algorithm than for the rigid (Fig. 1). Figure 2 shows a typical example of improved alignment with regard to tumor when a nonrigid algorithm was applied.

For CT during inspiration, fusion with ^{18}F-FDG PET was significantly improved by the use of nonlinear coregistration in 5 (lung apices, aortic arch, carina tracheae, sternum, and tumor) of 8 landmarks (supplemental table, available online only at http://jnm.snmjournals.org). For CT in expiration, comparison of the rigid and nonrigid algorithms demonstrated a significantly better fusion in 3 of 8 landmarks (lung apices, heart, and carina tracheae) in the nonrigid PET/CT dataset. Use of the mid-breath-hold CT scans resulted in significantly better fusion at the lung apices and carina tracheae in the nonrigid PET/CT dataset; on the other hand, fusion was significantly better at the tumor and heart in the rigid PET/CT dataset.

TABLE 1. Score for Assessment of Image Fusion Quality

Score	Finding
1	Complete lack of superimposition of anatomic structure on axial, coronal, and sagittal views
2	Difference in alignment of >25 mm
3	Difference in alignment of 5–25 mm
4	Difference in alignment of <5 mm
5	Excellent or complete superimposition of anatomic structure on axial, coronal, and sagittal views

Modified from (17).

TABLE 2. Comparison of Mean Fusion Quality of Nonrigid and Rigid Groups for Different Breathing Maneuvers

CT breathing maneuver	Rigid fusion	Nonrigid fusion	P
Inspiration	3.1 ± 0.7	3.3 ± 0.6	<0.001
Expiration	3.4 ± 0.7	3.6 ± 0.7	<0.001
Mid breath-hold	3.6 ± 0.7	3.5 ± 0.6	0.6
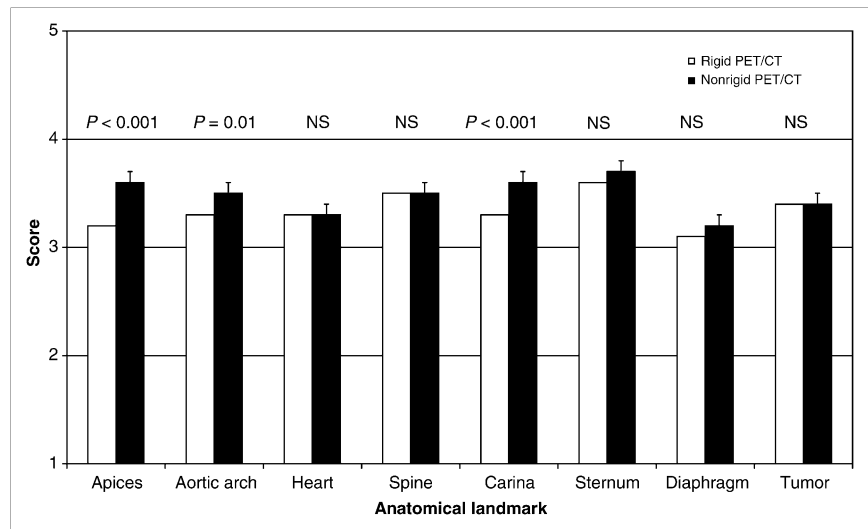
FIGURE 1. Differences between rigid PET/CT and nonrigid PET/CT datasets.

Inter- and Intraobserver Variability

Table 3 summarizes the degree of interobserver variability in the scoring of each anatomic landmark for both kinds of PET/CT fusion algorithms. Good overall agreement ($\kappa = 0.63$, $P < 0.001$) was found among the 3 reviewing physicians in the range between almost perfect to poor image fusion. Intraobserver variability for the rigid PET/CT dataset showed good agreement for each reviewer in reevaluation of fusion quality at each landmark. The interval between the analyses in this study and the previous work (14) was 1 y. Intraobserver variability was 0.56, 0.64, and 0.68, all these κ-values being significant ($P < 0.001$).

Breathing Maneuvers and Tumor Location

The breathing maneuvers were adequately performed in all 16 patients, as described in the prior report (14). No statistically significant difference in fusion quality was observed between centrally located tumors (10 patients) and peripheral tumors (6 patients). Furthermore, fusion quality did not significantly differ between upper-lobe lesions (9 patients) and lower-lobe lesions (7 patients).

DISCUSSION

To the best of our knowledge, this is the first analysis comparing linear and nonlinear registration algorithms for fusion of thoracic ^{18}F-FDG PET and CT images obtained with different breathing protocols in patients with non–small cell lung cancer. Our results clearly show that the fusion quality of ^{18}F-FDG PET and CT images strongly depends on the breathing maneuver performed during the CT acquisition, regardless of the algorithm used. Furthermore, the nonlinear algorithm clearly improves fusion quality when CT is performed during deep inspiration or expiration but not at mid breath-hold. In addition, our data clearly show the poor quality of fusion using CT scans that are acquired in deep inspiration and rigidly registered to PET scans, in comparison to those acquired at mid breath-hold. Thus, we recommend the combination of CT performed at mid breath-hold and nonrigid fusion with PET or, alternatively, nonrigidly fused end-expiration or end-inspiration CT with PET for routine display of fused PET/CT datasets.

The software used for the retrospective coregistration of CT and PET images was originally developed for research and clinical applications in brain imaging (25,26). Although with the advent of PET/CT many institutions do not perform retrospective fusion of PET and CT data, software fusion is not obsolete even for the data obtained on hybrid PET/CT machines (16,26). Especially in the case of integrated PET/CT, it is essential to correctly align PET and CT data before calculation of the attenuation map (16), which can be essential for staging, therapy response monitoring, or radiotherapy planning (21).

Up to now, rigid registration algorithms have been used to provide better alignment (13,14,17). Potential advantages have been proposed for nonrigid algorithms, which are thought to reduce misregistration errors, but a thorough clinical evaluation is still lacking. Our results confirmed our assumption that the nonrigid algorithms generally have a clear benefit for reaching the best fusion. However, in having a closer look at the data, we found a more complex situation than we had anticipated.

In the case of extreme breathing positions (i.e., full expiration or full inspiration), nonrigid algorithms achieve the most accurate alignment. The most likely explanation is that during tidal breathing (most clinical PET acquisitions are during shallow or tidal breathing), the position of the thoracic structures and upper abdomen on CT is anatomically closer to the mid-breath-hold position than to the full-expiration or -inspiration position.

Gilman et al. studied 5 breathing protocols (normal inspiration, normal expiration, small breath in, mid suspended breath-hold, and regular breathing) in 5 groups of patients (15) and found that the best fusion was reached
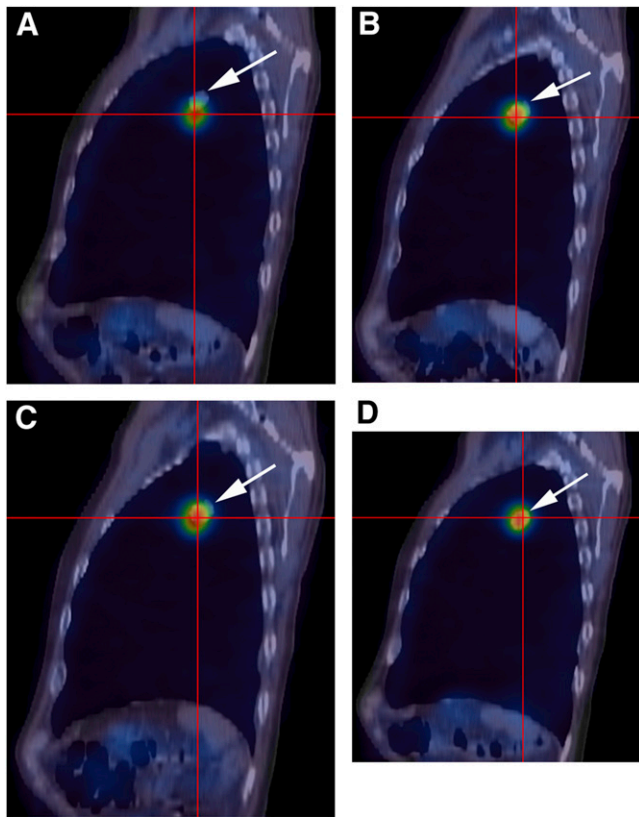
FIGURE 2. Fused PET/CT images of patient 7 with regard to tumor alignment. In rigidly registered PET/CT image during inspiration (A), alignment is poor between PET image (crosses) and CT image (arrows). (B and C) Almost exact alignment is seen in rigid PET/CT images at mid breath-hold (B) and during expiration (C). After nonrigid registration, alignment improves substantially during inspiration (D). Nonrigid expiration and nonrigid mid-breath-hold images (not shown) showed no change.

during normal expiration, a suspended breath-hold, or quiet breathing, concluding that additional software registration is not necessary (*15*). The use of nonlinear methods improved alignment discrepancies at the diaphragm using the inspiratory breathing methods (*15*). However, this group did not perform a strict intraindividual comparison.

TABLE 3. κ-Indices for Interobserver Agreement Among 3 Readers

	Rigid PET/CT		Nonrigid PET/CT	
Landmark	κ-Index	P	κ-Index	P
Lung apices	0.55	<0.001	0.66	<0.001
Aortic arch	0.64	<0.001	0.83	<0.001
Heart	0.59	<0.001	0.46	<0.001
Spine	0.62	<0.001	0.40	<0.001
Carina tracheae	0.67	<0.001	0.79	<0.001
Sternum	0.62	<0.001	0.59	<0.001
Diaphragm	0.61	<0.001	0.61	<0.001
Tumor	0.50	0.001	0.55	<0.001

In our study, we found improved alignment in lung apices, aortic arch, carina tracheae, sternum, and tumor using inspiratory CT and nonlinear methods. For expiratory CT, nonlinear methods resulted in better alignment at lung apices, heart, and carina tracheae.

Furthermore, the few studies performed to date were not performed strictly on patients with non–small cell lung cancer. Although Wolz et al. examined a heterogeneous patient population of 40 oncologic patients including 12 with lung cancer, only a single breathing maneuver was investigated (*27*). Recently, Moreno et al. published an interesting study with a new approach combining a breathing model and tumor-specific rigidity constraints for the registration of ^{18}F-FDG PET and CT data. However, the computational time for 1 dataset in that study requires more than 3 h even with modern computer hardware and thus currently cannot be implemented in the clinical routine (*28*).

Comparing our results with those of Gilman et al. (*15*), our alignment scores tend to be smaller. The most likely explanation might be the differences in fusion algorithms and imaging technology used. As discussed in our previous work, the alignment differences of up to 10 mm described by all 3 readers are twice the magnitude of a PET voxel (*14*). If we look at the sources of image registration errors, we see 2 main reasons. First, the technically achievable accuracy of the coregistration of 2 image datasets from separate modalities is limited. The magnitude of this kind of error was determined as being in the range of 2–3 mm (*29*), which was below the voxel dimensions of PET. Second, anatomic and structural variations due mainly to respiration and cardiac motion within the subject occur between the PET and CT acquisitions. The exact range of this kind of variation cannot be known unless the images undergo perfect fusion, which is currently impossible. Nevertheless, if full-inspiration or -expiration CT scans are used for the fusion with ^{18}F-FDG PET, nonrigid fusion algorithms can help reach acceptable fusion quality.

The present study showed good interreader agreement for the assessment of alignment quality (κ of 0.63), demonstrating the reproducibility of the score used. Furthermore, we found good intrareader reliability (κ of 0.62), indicating a homogeneous characterization of fusion quality across the 3 readers.

Our study had a few limitations. First, alignment might have been better on an integrated PET/CT scanner, and the breathing maneuvers might have been better on a CT scanner with more detector rows. However, the breathing maneuvers were correctly performed in this patient population. Second, our fusion score included only 5 grades. However, the assessment would have lost simplicity and reliability if the number of grades had been larger. Third, the use of another nonlinear algorithm might have shown different fusion results and have changed the conclusions. A further limitation is the retrospective nature of the study, including intrinsic selection bias and limited number of

patients. However, the study had strengths in the homogeneity of the patient population and its clinical importance.

The findings of this study are important for several clinical applications for hybrid PET/CT scanners. More accurate fusion is important for improvement of anatomic localization of diseases (*8*). During PET/CT, nonrigid misalignments still occur and could be corrected by nonlinear registration (*19*). In addition, retrospective nonrigid fusion may be necessary in serial comparison of PET/CT scans acquired at different times in the follow-up of oncologic patients. Finally, accurate registration of PET and CT images is crucial for PET-based radiotherapy planning, and nonrigid algorithms provide more accurate registration of PET/CT than does the rigid method (*30*).

CONCLUSION

Compared with rigid alignment algorithms, nonrigid registration of PET and CT data can significantly improve alignment if CT is performed during full inspiration or full expiration. If CT is performed at mid breath-hold, the use of rigid methods is warranted. Therefore, we recommend the use of nonrigid methods for image registration in the thorax if no mid-breath-hold CT scan is available to further improve the analysis of the images.

ACKNOWLEDGMENTS

REFERENCES

1. Jemal A, Thun MJ, Ries LA, et al. Annual report to the nation on the status of cancer, 1975-2005, featuring trends in lung cancer, tobacco use, and tobacco control. *J Natl Cancer Inst.* 2008;100:1672–1694.
2. Bilfinger TV. Surgical viewpoints for the definitive treatment of lung cancer. *Respir Care Clin N Am.* 2003;9:141–162.
3. Hellwig D, Baum RP, Kirsch C. FDG-PET, PET/CT and conventional nuclear medicine procedures in the evaluation of lung cancer: a systematic review. *Nuklearmedizin.* 2009;48:59–69.
4. Ukena D, Hellwig D. Value of FDG PET in the management of NSCLC. *Lung Cancer.* 2004;45 (suppl 2):S75–S78.
5. Halpern BS, Schiepers C, Weber WA, et al. Presurgical staging of non-small cell lung cancer: positron emission tomography, integrated positron emission tomography/CT, and software image fusion. *Chest.* 2005;128:2289–2297.
6. Aquino SL, Asmuth JC, Alpert NM, Halpern EF, Fischman AJ. Improved radiologic staging of lung cancer with 2-[^{18}F]-fluoro-2-deoxy-D-glucose-positron emission tomography and computed tomography registration. *J Comput Assist Tomogr.* 2003;27:479–484.
7. Beyer T, Townsend DW, Brun T, et al. A combined PET/CT scanner for clinical oncology. *J Nucl Med.* 2000;41:1369–1379.
8. Beyer T, Antoch G, Blodgett T, Freudenberg LF, Akhurst T, Mueller S. Dual-modality PET/CT imaging: the effect of respiratory motion on combined image quality in clinical oncology. *Eur J Nucl Med Mol Imaging.* 2003;30:588–596.
9. Gould KL, Pan T, Loghin C, Johnson NP, Guha A, Sdringola S. Frequent diagnostic errors in cardiac PET/CT due to misregistration of CT attenuation and emission PET images: a definitive analysis of causes, consequences, and corrections. *J Nucl Med.* 2007;48:1112–1121.
10. Nehmeh SA, Erdi YE, Ling CC, et al. Effect of respiratory gating on quantifying PET images of lung cancer. *J Nucl Med.* 2002;43:876–881.
11. Schaefer A, Kremp S, Hellwig D, Rube C, Kirsch CM, Nestle U. A contrast-oriented algorithm for FDG-PET-based delineation of tumour volumes for the radiotherapy of lung cancer: derivation from phantom measurements and validation in patient data. *Eur J Nucl Med Mol Imaging.* 2008;35:1989–1999.
12. Goerres GW, Kamel E, Heidelberg TN, Schwitter MR, Burger C, von Schulthess GK. PET-CT image co-registration in the thorax: influence of respiration. *Eur J Nucl Med Mol Imaging.* 2002;29:351–360.
13. Gilman MD, Fischman AJ, Krishnasetty V, Halpern EF, Aquino SL. Optimal CT breathing protocol for combined thoracic PET/CT. *AJR.* 2006;187:1357–1360.
14. Grgic A, Nestle U, Schaefer-Schuler A, Kremp S, Kirsch CM, Hellwig D. FDG-PET-based radiotherapy planning in lung cancer: optimum breathing protocol and patient positioning—an intraindividual comparison. *Int J Radiat Oncol Biol Phys.* 2009;73:103–111.
15. Gilman MD, Fischman AJ, Krishnasetty V, Halpern EF, Aquino SL. Hybrid PET/CT of the thorax: when is computer registration necessary? *J Comput Assist Tomogr.* 2007;31:395–401.
16. Weigert M, Pietrzyk U, Muller S, Palm C, Beyer T. Whole-body PET/CT imaging: combining software- and hardware-based co-registration. *Z Med Phys.* 2008;18:59–66.
17. Krishnasetty V, Fischman AJ, Halpern EL, Aquino SL. Comparison of alignment of computer-registered data sets: combined PET/CT versus independent PET and CT of the thorax. *Radiology.* 2005;237:635–639.
18. Lamare F, Cresson T, Savean J, Cheze Le Rest C, Reader AJ, Visvikis D. Respiratory motion correction for PET oncology applications using affine transformation of list mode data. *Phys Med Biol.* 2007;52:121–140.
19. Shekhar R, Walimbe V, Raja S, et al. Automated 3-dimensional elastic registration of whole-body PET and CT from separate or combined scanners. *J Nucl Med.* 2005;46:1488–1496.
20. Slomka PJ, Dey D, Przetak C, Aladl UE, Baum RP. Automated 3-dimensional registration of stand-alone ^{18}F-FDG whole-body PET with CT. *J Nucl Med.* 2003;44:1156–1167.
21. Bridges RL. Software fusion: an option never fully explored. *J Nucl Med.* 2009;50:834–836.
22. Wolz G, Nomayr A, Hothorn T, et al. Anatomical accuracy of interactive and automated rigid registration between x-ray CT and FDG-PET. *Nuklearmedizin.* 2007;46:43–48.
23. Fitton I, Steenbakkers RJ, Gilhuijs K, et al. Impact of anatomical location on value of CT-PET co-registration for delineation of lung tumors. *Int J Radiat Oncol Biol Phys.* 2008;70:1403–1407.
24. Fleiss J. *Statistical Methods for Rates and Proportions.* 2nd ed. New York, NY: Wiley; 1981.
25. Pelizzari CA, Chen GT, Spelbring DR, Weichselbaum RR, Chen CT. Accurate three-dimensional registration of CT, PET, and/or MR images of the brain. *J Comput Assist Tomogr.* 1989;13:20–26.
26. Pietrzyk U. Does PET/CT render software registration obsolete? *Nuklearmedizin.* 2005;44(suppl 1):S13–S17.
27. Wolz G, Nömayr A, Hothorn T, et al. Comparison of performance between rigid and non-rigid software registering CT to FDG-PET. *Int J CARS.* 2007;2:183–190.
28. Moreno A, Chambon S, Santhanam AP. Combining a breathing model and tumor-specific rigidity constraints for registration of CT-PET thoracic data. *Comput Aided Surg.* 2008;13:281–298.
29. West J, Fitzpatrick JM, Wang MY, et al. Comparison and evaluation of retrospective intermodality brain image registration techniques. *J Comput Assist Tomogr.* 1997;21:554–566.
30. Ireland RH, Dyker KE, Barber DC, et al. Nonrigid image registration for head and neck cancer radiotherapy treatment planning with PET/CT. *Int J Radiat Oncol Biol Phys.* 2007;68:952–957.